Subspace Methods for Frequency Domain Data

Tomas McKelvey

Abstract— **Subspace based methods for system identification have, during the last 10 years, matured and been accepted as important tools. Subspace based methods deliver the estimate directly in the form of a state-space realization. This is an advantage as many model based control design techniques use state-space models. Subspace algorithms have been formulated for use of both time domain as well as frequency domain data. In this tutorial contribution the class of frequency domain algorithms will be covered. Frequency domain subspace methods have been very accurate for the estimation of transfer functions of systems with a high modal density and/or poorly damped modes. The basic algorithmic structure for a frequency domain algorithm will be derived. Also the numerical implementation using QR-factorization and singular value decomposition will be covered. Several examples will be provided including identification of flexible structures, and modeling of an acoustic path.**

I. Introduction

System identification deals with estimating models of a dynamical system based on input and output data records. In this paper we will deal with the black box identification problem where a non-structured time-invariant rational transfer function of finite order is estimated from the data.

Identification algorithms which identify state-space models by means of a subspace approximation are commonly known as subspace methods and have received much attention in the literature. The early subspace identification methods [1], [2], [3], [4] are based on time-domain data. An nice overview of time domain subspace methods is given by [5]. One of the advantages with subspace methods is the absence of a parametric iterative optimization step. In classical prediction error minimization [6], such a step is necessary for most model structures. A second advantage is that the identification of multivariable systems is just as simple as for scalar systems. Particularly one do not have to deal with the parametrization issue of multivariable systems since no explicit parametrization is needed.

In this paper we consider the case when data is given in the frequency domain, i.e., when samples of the Fourier transform of the input and output signals are the primary measurements. In a number of applications, particularly when modeling flexible structures, it is common to fit the data to models in the frequency domain [7], [6]. A few subspace based algorithms formulated in the frequency domain has appeared in the literature [8], [9], [10], [11]. The aim of this paper is to, in a tutorial fashion, describe a frequency domain subspace method based on the methods presented in [9], [10].

This work was sponsored by the Swedish Research Council (VR) which is gratefully acknowledged

T. McKelvey is with the Department of Signals and Systems, Chalmers University of Technology, SE-412 96 Göteborg, Sweden, mckelvey@s2.chalmers.se

A. State-space models

State-space models is an attractive model class to represent rational transfer functions. A discrete-time state-space model can be written as

$$\begin{aligned} x(k+1) &= Ax(k) + Bu(k) \\ y(k) &= Cx(k) + Du(k) + v(k) \end{aligned} \tag{1}$$

where $x(k) \in \mathbb{R}^n$ is the state-vector, $u(k) \in \mathbb{R}^m$ is the vector of inputs, $y(k) \in \mathbb{R}^p$ is the vector of outputs and $v(k) \in \mathbb{R}^p$ is a vector of noise and/or model errors. Here the index k denotes sample number and if the data is sampled with a sampling period T_s, $u(k)$ is the sample of the input at time instant $t = kT_s$. The matrices A, B, C and D forms the realization of the transfer function and have dimensions such that the vector matrix multiplications in (1) are all well defined, e.g. the matrix A has n rows and n columns. We also assume that the realization is minimal [12] and hence the McMillan degree of the system equals the length of the state-vector.

With the standard definition of the discrete-time Fourier transform (DTFT) of a sequence $x(k)$

$$\mathrm{DTFT}\{x(k)\} \triangleq X(\omega) \triangleq \sum_{k=-\infty}^{\infty} x(k) e^{-j\omega k} \tag{2}$$

it is obvious that $\mathrm{DTFT}\{x(k+r)\} = e^{j\omega r} X(\omega)$. Applying the DTFT to (1) yields

$$\begin{aligned} e^{j\omega} X(\omega) &= AX(\omega) + BU(\omega) \\ Y(\omega) &= CX(\omega) + DU(\omega) + V(\omega) \end{aligned} \tag{3}$$

and finally, if eliminating $X(\omega)$ from above and set $V(\omega) = 0$ we obtain

$$\begin{aligned} Y(\omega) &= \left(D + C(e^{j\omega} I - A)^{-1} B\right) U(\omega) \\ &\triangleq G(e^{j\omega}) U(\omega). \end{aligned} \tag{4}$$

Here $G(z)$ is the transfer function which in general is a matrix with rational functions as matrix elements.

Although all data used for calculations is sampled by nature it is in some cases the underlying continuous-time system which it is desirable to model. A continuous-time state-space model can be written as

$$\begin{aligned} \dot{x}^c(t) &= A^c x^c(t) + B^c u(t) \\ y(t) &= C^c x^c(t) + D^c u(t) + v(t) \end{aligned} \tag{5}$$

with the corresponding transfer function $G^c(s) = D^c + C^c(sI - A^c)^{-1} B^c$. In Section IV we will further discuss how to estimate continuous-time models using the subspace tools for discrete-time models.

B. Identification problem

Assume we have data from the system in terms of samples of the Fourier transform of the input $U_k = U(\omega_k)$ and output signals $Y_k = Y(\omega_k)$ at a set of M frequencies ω_k. Then the goal is to find a transfer function in the form of a state-space realization $(\hat{A}, \hat{B}, \hat{C}, \hat{D})$ from the given data.

II. Frequency data

Frequency data in the form of $Y(\omega_k)$ and $U(\omega_k)$ can in principle be obtained in two different ways.

- Through a frequency testing procedure which produces samples of the frequency response function (FRF), so called FRF-data.
- By directly recording time domain samples of the input and output and subsequently use the discrete Fourier transform (DFT) to convert them to the frequency domain.

Procedures for obtaining FRF-data, $\hat{G}_r$, normally involves careful selection of input signals, long measurement times and averaging techniques to suppress measurement noise. Hence FRF-data has a high SNR. From the estimated matrices $\hat{G}_r$ an input-output data set is formed as follows: For each FRF frequency sample $r = 0, \ldots, N-1$ and for each input $l = 1, \ldots, m$ let Y_{r*m+l} be column l of matrix G_r and let $U_{r*m+l} = e_l$ where e_l is column l of the $m \times m$ identity matrix. Hence, a set of N FRF-data matrices yields a total of $M = N * m$ input-output data pairs. Each frequency and column in $\hat{G}_k$ thus contributes to one input-output pair $\{Y_k, U_k\}$. The reason for re-shaping the data is to facilitate the use of the same algorithms for both FRF-data as well as directly measured input-output data.

The second alternative to obtain frequency data is to employ the raw DFT to the recorded input and output data sequences. In general for N data samples the relation between the model and the frequency data are for the DFT frequency grid $\omega_k = 2\pi k/N, k = 0, \ldots, N-1$ given by [13]

$$Y_k = \left[\begin{bmatrix} D & 0 \end{bmatrix} + C(e^{j\omega_k} I - A)^{-1} \begin{bmatrix} B & P \end{bmatrix}\right] \begin{bmatrix} U_k \\ e^{j\omega_k} \end{bmatrix} \tag{6}$$

where the extra term P captures the dependence on the initial state $x(0)$ and final state $x(N)$. If $x(0) = x(N)$, which is the case if a periodic input is used with period time N and the system has reached a stationary periodic operation, then $P = 0$. If data is periodic the extra term can be discarded. If data is not periodic the extra vector P should be estimated along with the system by simply augmenting the input vector to become $\begin{bmatrix} U_k \\ e^{j\omega_k} \end{bmatrix}$.

III. Subspace estimation method

In this section we will discuss how a state-space realization can be estimated using frequency domain data. Throughout the derivation we will assume noise free data $V(\omega_k) = 0$ and we will discuss the influence of the noise at the end of the section.

A. Vector relations

First consider the case where delayed outputs and inputs are stacked. With use of (1) it is easy to see that

$$\begin{bmatrix} y(k) \\ y(k+1) \\ \vdots \\ y(k+q-1) \end{bmatrix} = \mathcal{O}x(k) + \Gamma \begin{bmatrix} u(k) \\ u(k+1) \\ \vdots \\ u(k+q-1) \end{bmatrix} \tag{7}$$

where $\mathcal{O}$ is the extended observability matrix with $q \geq n$ block rows

$$\mathcal{O} = \begin{bmatrix} C \\ CA \\ \vdots \\ CA^{q-1} \end{bmatrix} \tag{8}$$

and Γ is a lower block-triangular Toeplitz matrix with the structure

$$\Gamma = \begin{bmatrix} D & 0 & \ldots & 0 \\ CB & D & \ldots & 0 \\ \vdots & \vdots & \ddots & \vdots \\ CA^{q-2}B & CA^{q-3}B & \ldots & D \end{bmatrix}. \tag{9}$$

An application of the DTFT to (7) results in the vector relation

$$\begin{bmatrix} Y(\omega) \\ Y(\omega)e^{j\omega} \\ \vdots \\ Y(\omega)e^{j\omega(q-1)} \end{bmatrix} = \mathcal{O}X(\omega) + \Gamma \begin{bmatrix} U(\omega) \\ U(\omega)e^{j\omega} \\ \vdots \\ U(\omega)e^{j\omega(q-1)} \end{bmatrix} \tag{10}$$

which holds for all ω. Using all data samples at the frequencies ω_k for $k = 0, \ldots, M-1$, we can merge all the M vector relations into

$$\boldsymbol{Y} = \mathcal{O}\boldsymbol{X} + \Gamma\boldsymbol{U} \tag{11}$$

where column k in (11) corresponds to (10) for $\omega = \omega_k$. The number of block-rows in $\boldsymbol{Y}$ is controlled by the auxiliary order q. Since the realization is assumed minimal, the matrix $\mathcal{O}$ defined in (8) has full rank n whenever $q \geq n$, see [12]. Hence, the matrix product $\mathcal{O}\boldsymbol{X}$ has at most rank n. The output $\boldsymbol{Y}$ is thus composed of the sum of a low-rank matrix and (in general) a full rank matrix $\Gamma\boldsymbol{U}$. Since the number of columns in (11) equals the number of data, the matrices become wider as M increases. Let us introduce the notation $\boldsymbol{Y}^{\mathrm{re}} \triangleq [\mathrm{Re}\,\boldsymbol{Y},\ \mathrm{Im}\,\boldsymbol{Y}]$. Since the state-space realization (A, B, C, D) has real-valued matrices, the complex matrix expression (11) can be equivalently be formulated as

$$\boldsymbol{Y}^{\mathrm{re}} = \mathcal{O}\boldsymbol{X}^{\mathrm{re}} + \Gamma\boldsymbol{U}^{\mathrm{re}} \tag{12}$$

which is the basic equation many subspace based system identification methods use, see e.g. [5], [8], [9]. In (12) note that only the matrices $\boldsymbol{Y}^{\mathrm{re}}$ and $\boldsymbol{U}^{\mathrm{re}}$ are known.

B. Key steps

The subspace method can be divided into four distinct steps:

1) To remove the influence of the term $\Gamma \boldsymbol{U}^{\mathrm{re}}$
2) To estimate the range space of the matrix $\mathcal{O}\boldsymbol{X}^{\mathrm{re}}$
3) From the estimated range space calculate $\hat{A}$ and $\hat{C}$
4) Use $\hat{A}$ and $\hat{C}$ to estimate $\hat{B}$ and $\hat{D}$

Let us denote by $\boldsymbol{\Pi}^{\perp}$ a matrix which projects onto the null space of $\boldsymbol{U}^{\mathrm{re}}$ and multiply this matrix from the right in (12). Since $\boldsymbol{U}^{\mathrm{re}}\boldsymbol{\Pi}^{\perp} = 0$ we directly obtain $\boldsymbol{Y}^{\mathrm{re}}\boldsymbol{\Pi}^{\perp} = \mathcal{O}\boldsymbol{X}^{\mathrm{re}}\boldsymbol{\Pi}^{\perp}$. A numerically efficient and stable way to perform this step is by using a QR-factorization [14]

$$\begin{bmatrix} \boldsymbol{U}^{\mathrm{re}T} & \boldsymbol{Y}^{\mathrm{re}T} \end{bmatrix} = \begin{bmatrix} Q_1 & Q_2 \end{bmatrix} \begin{bmatrix} R_{11} & R_{12} \\ 0 & R_{22} \end{bmatrix} \quad (13)$$

and noting that $\boldsymbol{Y}^{\mathrm{re}}\boldsymbol{\Pi}^{\perp} = R_{22}^T Q_2^T$. In the next step a basis of the range space of $\mathcal{O}$ is estimated. The singular value decomposition (SVD) is used for this purpose [14]

$$R_{22}^T = \begin{bmatrix} U_s & U_o \end{bmatrix} \begin{bmatrix} \Sigma_s & 0 \\ 0 & \Sigma_o \end{bmatrix} \begin{bmatrix} V_s^T \\ V_o^T \end{bmatrix}. \quad (14)$$

where $[U_s,\ U_o]$ and $[V_s,\ V_o]$ are two square orthonormal matrices and Σ_s and Σ_o are diagonal matrices with non-negative entries sorted such that all diagonal entries in Σ_s are larger then the ones in Σ_o and the dimension of Σ_n is selected to be $n \times n$. The diagonal entries in Σ_s and Σ_o are called the singular values. The rank of a matrix can be determined by calculating the number of non-zero singular values. In our case $\operatorname{rank} R_{22} = \operatorname{rank}(\boldsymbol{Y}^{\mathrm{re}}\boldsymbol{\Pi}^{\perp}) \leq \operatorname{rank}\mathcal{O} = n$, i.e., the rank can at most be n. This implies that $\Sigma_o = 0$. It can be shown that the projection does not decrease the rank any further [9] so in fact $\operatorname{rank} R_{22} = n$ and hence all n singular values in Σ_n are positive. Therefore $R_{22}^T = U_s\Sigma_s V_s^T$ and as an estimate of the extended observability matrix we use $\hat{\mathcal{O}} = U_s$. If we set $T = \boldsymbol{X}^{\mathrm{re}}\boldsymbol{\Pi}^{\perp}Q_2 V_s \Sigma_s^{-1}$ it is straightforward to verify that $\hat{\mathcal{O}} = U_s = \mathcal{O}T$. Here it is important to point out that only the range space of $\mathcal{O}$ has been calculated. The range space information is however enough to recover the transfer function in *some* realization.

Consider a state-space realization $(A_T, B_T, C_T, D_T) = (T^{-1}AT, T^{-1}B, CT, D)$ for a non-singular square matrix T. The transfer function of the transformed realization (A_T, B_T, C_T, D_T) is equal to the transfer function of (A, B, C, D) and the two realizations are called *similar* [12]. A similarity transformation with a matrix T changes the extended observability matrix according to $\mathcal{O}_T = \mathcal{O}T$. The estimate $\hat{\mathcal{O}}$ derived above is thus exactly an extended observability matrix of a realization similar to the original one.

The estimates of $\hat{A}$ and $\hat{C}$ are now immediate. Firstly $\hat{C}$ is taken as the first p rows of $\hat{\mathcal{O}}$. Secondly if we define $\overline{\hat{\mathcal{O}}}$ as the matrix obtained from $\hat{\mathcal{O}}$ by removing the top p rows and define $\underline{\hat{\mathcal{O}}}$ as the matrix obtained by removing the bottom p rows it is clear from (8) that $\underline{\hat{\mathcal{O}}}\hat{A} = \overline{\hat{\mathcal{O}}}$. The matrix $\underline{\hat{\mathcal{O}}}$ has $q - 1 \geq n$ block rows and has, as argued previously, full rank. The state-transition matrix is then obtained by

$$\hat{A} = \underline{\hat{\mathcal{O}}}^{+}\overline{\hat{\mathcal{O}}} \quad (15)$$

where the notation $(\cdot)^+$ denotes the pseudo-inverse of a matrix [14].

In the fourth and final step the $\hat{B}$ and $\hat{D}$ matrices are calculated by solving a set of linear equations. Let $\operatorname{vec} X$ denote the vector obtained by stacking, in order from left to right, the columns of the matrix X. In particular if x is a vector then $\operatorname{vec} x = x$. From (4), the use of the Kronecker product $\otimes$ and the identity $\operatorname{vec}(ABC) = (C^T \otimes A)\operatorname{vec} B$, see [15], we obtain

$$\begin{aligned} Y_k &= \begin{bmatrix} I & \hat{C}(e^{j\omega_k}I - \hat{A})^{-1} \end{bmatrix} \begin{bmatrix} \hat{D} \\ \hat{B} \end{bmatrix} U_k \\ &= \underbrace{\left(U_k^T \otimes \begin{bmatrix} I & \hat{C}(e^{j\omega_k}I - \hat{A})^{-1} \end{bmatrix}\right)}_{\Psi_k} \underbrace{\operatorname{vec}\begin{bmatrix} \hat{D} \\ \hat{B} \end{bmatrix}}_{\hat{\theta}} \quad (16) \\ &= \Psi_k \hat{\theta} \end{aligned}$$

for $k = 0, \ldots, M-1$. Again we are interested in a solution which is real-valued so we stack the real and imaginary parts of the equation above. With the notation $X^{\mathrm{rs}} \triangleq \left[\begin{smallmatrix} \operatorname{Re} X \\ \operatorname{Im} X \end{smallmatrix}\right]$ we obtain $Y_k^{\mathrm{rs}} = \Psi_k^{\mathrm{rs}}\hat{\theta}$. The B and D elements are then obtained from by solving $\hat{\theta}$ from the normal equations

$$\sum_{k=0}^{M-1} \Psi_k^{\mathrm{rs}T} Y_k^{\mathrm{rs}} = \left(\sum_{k=0}^{M-1} \Psi_k^{\mathrm{rs}T}\Psi_k^{\mathrm{rs}}\right)\hat{\theta}. \quad (17)$$

C. Noise and under-modeling

In any realistic case the measurement error $V(\omega)$ is non-zero. The origin of this error can be traced to two sources: random measurement errors and systematic errors due to the fact that a finite dimensional transfer function of McMillan degree n is not flexible enough to capture the underlying system. In the method outlined above the errors are suppressed by the SVD step (14), in the calculation of $\hat{A}$, and finally when calculating $\hat{B}$ and $\hat{D}$ (17). Due to the influence from $V(\omega)$, the matrix $\boldsymbol{Y}^{\mathrm{re}}\boldsymbol{\Pi}^{\perp}$ will in general have full rank. The SVD calculation of $\hat{\mathcal{O}}$ is the optimal solution to

$$\min_{\mathcal{O},Z} \|\mathcal{O}Z - \boldsymbol{Y}^{\mathrm{re}}\boldsymbol{\Pi}^{\perp}\|_2^2$$

where the matrix norm is the induced 2-norm [14]. This means that the SVD provides us with the optimal $\operatorname{rank} n$ approximation. In the noise-free case the number of positive singular values equals the McMillan degree of the transfer function. If the model order is unknown the number of large singular values can be used as a guide for selecting an appropriate model order. In [9] and [16] further analysis are given. The calculation of $\hat{A}$ in (15) is the solution to a least-squares problem:

$$\min_{A} \|\underline{\hat{\mathcal{O}}}A - \overline{\hat{\mathcal{O}}}\|_F^2$$

where the matrix norm is the Frobenius norm $\|X\|_F^2 = \operatorname{vec}(X)^T \operatorname{vec}(X)$. As an alternative to the least-squares solution one can also consider using the total-least-squares (TLS) solution [14] since both $\underline{\hat{\mathcal{O}}}$ and $\overline{\hat{\mathcal{O}}}$ are subject to

errors. Finally the $\hat{B}$ and $\hat{D}$ calculation (17) is also the solution to the least-squares problem

$$\min_{\theta} \sum_{k=0}^{M-1} \|Y_k^{\mathrm{rs}} - \Psi_k^{\mathrm{rs}}\theta\|^2. \tag{18}$$

Alternatively one could use TLS since Ψ_k^{rs} is based on the estimated $\hat{A}$ and $\hat{C}$ and is thus subject to some errors.

To shape the errors in this last step it can be beneficial to include a frequency dependent weighting W_k

$$\min_{\theta} \sum_{k=0}^{M-1} \|W_k(Y_k^{\mathrm{rs}} - \Psi_k^{\mathrm{rs}}\theta)\|^2. \tag{19}$$

The weighting matrix W_k can be chosen based on the statistical properties on the noise, see below.

D. Pre-processing

In all numerical procedures it is important to make sure that the data is balanced in the sense that different channels in the input and output has compatible sizes. Using unbalanced data can seriously degrade the accuracy of the method. One possibility is to scale the data such that each input and output channel has unit power and use the rescaled data sets for identification.

E. Choice of weightings

If we assume $V(\omega_k)^{\mathrm{rs}}$ to be a zero mean stochastic variable with covariance

$$R_k = \mathrm{E}\{V(\omega_k)^{\mathrm{rs}} V(\omega_k)^{\mathrm{rs}T}\} \tag{20}$$

then W_k in (19) should be selected as $W_k = R_k^{-1/2}$ where $R_k^{-1/2}$ is the inverse of the matrix square root of R_k, i.e., $R_k^{-1/2} R_k (R_k^{-1/2})^T = I$. This gives the minimum variance estimate of $\hat{B}$ and $\hat{D}$ if we disregard any estimation errors in $\hat{A}$ and $\hat{C}$.

Also the subspace equations (11) can be weighted based on the noise characteristic. Each column in (11) represents one frequency ω_k and can individually be rescaled by an arbitrary non-zero scalar. If a single output model is estimated the column k in (11) should be multiplied by $R_k^{-1/2}$ (which in the single output case is a scalar). For the multiple output case the scalar can be chosen as $(\mathrm{tr}(R_k)/p)^{-1/2}$ which is based on the average covariance over all the output channels. For a deeper discussion on weightings and stochastic convergence analysis we refer to [9], [16].

When FRF-data is used for identification, the data often has a high SNR and most misfit between the model and data are due to the restrictiveness of the finite order model, i.e., the error is unmodeled dynamics. In such case the weightings can be used to shape the model error to suit the usage of the final estimated model. If the model is required to have a good fit at a certain portion of the frequency response, the corresponding noise variances should be made small to obtain a higher weighting at those frequencies. Of course the improved fit at the selected frequencies would normally imply that the error would increase elsewhere. Often a procedure must be employed where models are estimated and evaluated and new weightings are constructed in an iterative fashion.

F. Choice of auxiliary order

The number of block rows q in $\boldsymbol{Y}$ and $\boldsymbol{U}$ needs to be selected. A strict requirement is that $q \geq n$ in order to obtain identifiability. Numerical experience has shown that if the identified system has modes with a low damping it is beneficial to select a high value for q sometimes as high as $q = 10n$. For systems with well damped modes increasing q from gives no extra accuracy. The behavior can partly be explained by the structure of the extended observability matrix, where the block rows contain increasing powers of the matrix A. Clearly, if the system only has well damped modes A^{q-1} will be close to zero even for moderate values of q while for modes with less damping the converse is true.

IV. Handling continuous-time models

A straight forward application of the subspace ideas in a continuous-time setting immediately results in severe numerical problems since high powers of $j\omega$ would be used. Two alternative routes exists to circumvent this problem. In [11] a continuous-time algorithm is presented using a special recursive technique which avoids the numerical ill-conditioning. Here, a second alternative is reviewed which reformulates the continuous-time problem to a discrete-time one and hence, the standard discrete-time estimation tools can be used without modification [9]. To achieve this we use the properties of the bilinear-transformation defined through the equation

$$s = \frac{2(z-1)}{T(z+1)} \tag{21}$$

where s is the Laplace variable and z is the Z-transform variable. The scalar T can be interpreted as a sampling period but serves the purpose to rescale the frequencies, see further below. Let $G^c(s)$ represent a continuous-time transfer function and define a discrete-time transfer function as

$$G(z) \triangleq G^c(s)|_{s=\frac{2(z-1)}{T(z+1)}} = G^c(\frac{2(z-1)}{T(z+1)}) \tag{22}$$

Let (A^c, B^c, C^c, D^c) be a state-space realization of $G^c(s)$. Then (A, B, C, D) will be be a realization of $G(z)$ where [17]

$$\begin{aligned} A =& (\frac{2}{T}I + A^c)(\frac{2}{T}I - A^c)^{-1} \\ B =& \frac{2}{\sqrt{T}}(\frac{2}{T}I - A^c)^{-1}B^c \\ C =& \frac{2}{\sqrt{T}}C^c(\frac{2}{T}I - A^c)^{-1} \\ D =& D^c + C^c(\frac{2}{T}I - A^c)^{-1}B^c \end{aligned} \tag{23}$$

which also imply

$$\begin{aligned} A^c =& \frac{2}{T}(I + A)^{-1}(A - I) \\ B^c =& \frac{2}{\sqrt{T}}(I + A)^{-1}B \\ C^c =& \frac{2}{\sqrt{T}}C(I + A)^{-1} \\ D^c =& D - C(I + A)^{-1}B. \end{aligned} \tag{24}$$

Clearly, the state-dimension is unchanged by the transformation. Furthermore the frequency responses of the two transfer functions are linked as

$$G^c(j\Omega) = G(e^{j\omega}), \quad \text{if} \quad T\Omega = 2\tan(\omega/2) \tag{25}$$

The bilinear transformation compresses the entire continuous-time frequency scale $\Omega \in [0, \infty]$ to the finite discrete-time counterpart $\omega \in [0, \pi]$. The relation $T\Omega = 2\tan(\omega/2)$ is often called frequency warping.

A. Estimation strategy

Assume input/output data samples are given at the continuous-time frequencies Ω_k. The necessary steps for the identification of a continuous-time transfer function are:

1) Select an appropriate value of T the frequency scaling. As a rule of thumb a value of $T = 5/\max_k \Omega_k$ can be used.
2) Associate the given input-output pair at frequency Ω_k with the discrete-time frequency

$$\omega_k = 2\,\mathrm{atan}(T\Omega_k/2) \tag{26}$$

3) From the input/output data and frequencies ω_k estimate a discrete-time state-space model using appropriate tools.
4) Use the relation (24) to obtain the final continuous-time state-space realization.

It should be noted that the conversion to discrete-time and back is exact and hence do not introduce any systematic errors or approximations.

V. Examples

A. Cantilever beam

In this example the dynamics of a cantilever beam is identified. The beam is equipped with three actuators and three sensors. The three actuators are of piezo-electric type and they produce a bending force when charge is applied them. The first sensor measures the deflection of the tip using a touch-free laser-interferometry technique. The second and third sensors are of piezo-electric type and co-located with the second and third actuator.

Frequency response function data is produced by performing three experiments, one for each actuator using a periodic input excitation and averaging. The data covers a linear frequency grid of 2542 points between 5 and 163 Hz. The FRF data is converted to the I/O form according to the description in Section II. A three inputs three outputs MIMO continuous-time model is requested so the data is converted to discrete-time by rescaling the frequency axis using $T = 2 \times 10^{-1}$, see (26) for details. A preliminary estimation, without any weights applied, of a 7th order model ($n = 7$) and auxiliary order selected as $q = 100$, revealed that all spectral peaks were well identified. However, some of the zero locations, i.e., the notches in the frequency response were not as well reproduced. To improve the fit around the zero locations extra weightings were applied at the zero frequency locations for the first subspace step. In the LS estimation of B and D matrices, weighting was only applied to those channels (of the total of 9) which needed extra attention. A re-estimation with the applied weights gave satisfactory results and the final continuous time state-space model was calculated from the equations (24). Two of the nine estimated transfer functions are presented in Figures 1 and 2 together with the FRF-data and the error between the model and the FRF-data. The other seven transfer functions were also of similar quality.

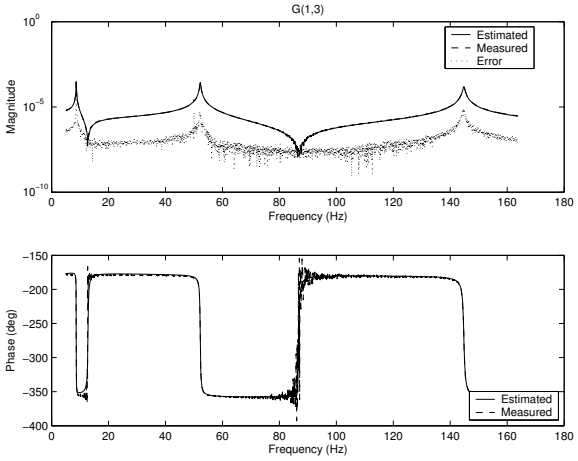

Fig. 1. Cantilever beam transfer function between input 3 and output 1. Solid line - model, Dashed line FRF-data and dashed line error between model and FRF-data.

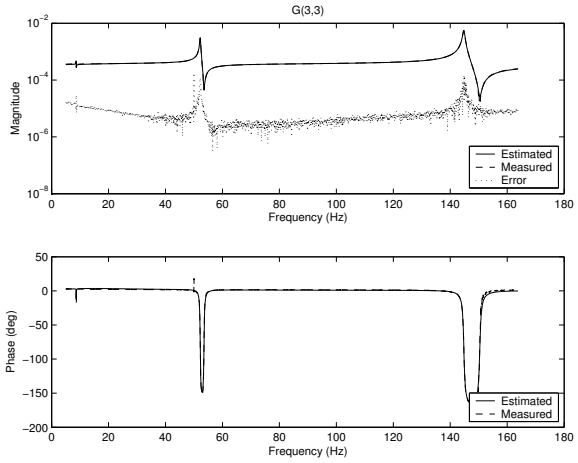

Fig. 2. Cantilever beam transfer function between input 3 and output 3. Solid line - model, Dashed line FRF-data and dashed line error between model and FRF-data.

B. ARC testbed

This application considers the identification of the transfer function between a force-actuator and an accelerometer located on a flexible mechanical structure. The structure is the Advanced Reconfigurable Control (ARC) testbed at the Jet Propulsion Laboratory (JPL), California Institute of Technology, Pasadena, California.

The frequency data are obtained with a sampling frequency of 200 Hz using a multi-sine input [7] with 512 equidistant spectral lines. This data has a large number of flexible modes and a SISO continuous-time model of order 70 is estimated from the data using the frequency domain-subspace algorithm with auxiliary order $q = 500$.

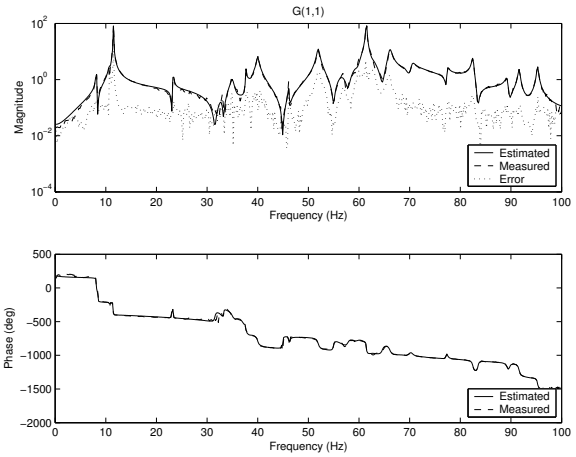

Fig. 3. Transfer function between force and accelerometer in the ARC testbed. Solid line - model, Dashed line - FRF-data and dotted line - error between model and FRF-data.

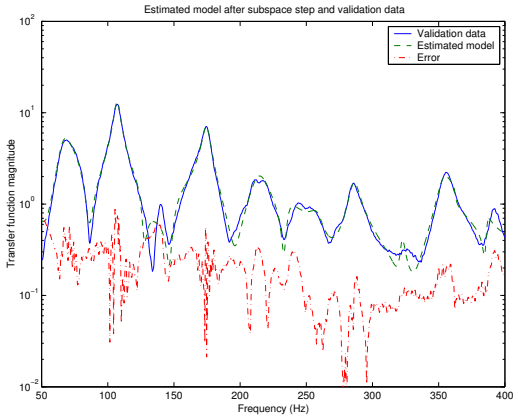

Fig. 4. Magnitude transfer functions of parametric model estimate of order 29 from subspace algorithm and ETFE from validation data. The magnitude of the error also is shown. The transfer functions are derived from the applied actuator voltage to measured microphone preamp voltage. (-) Validation Data, (- -) Estimated model, (– -) Error.

The frequency response data together with the response of the estimated model are shown in Figure 3.

C. Acoustic duct

In this application the transfer function between a speaker and a microphone mounted in an acoustic duct is estimated. The experimental input-output time series is divided into two equal size data sets, one estimation set and another set for validation purposes. The estimation data is transformed to the frequency domain by use of the fast Fourier transform (FFT) without any windowing functions. A subset if the data is selected which leads to an identification set with 1545 points with a high SNR. The subspace estimation algorithm is employed to estimate a model of order 29 using $q = 60$ as the auxiliary order. The result can be studied in Figure 4. The identification result can significantly be improved by employing a nonlinear optimization step, see [10] for more details. Hence, a good strategy is to combine the subspace based method with a subsequent non-linear optimization of the frequency-domain prediction error, see e.g. [18].

VI. Acknowledgments

The author would like thank Prof. L. Ljung for arranging this invited session and Prof. Reza Moheimani, Dr. Andrew Fleming and Mr. Benjamin Vautier, University of Newcastle, Australia for providing the cantilever beam and acoustic duct data. The author is also indebted to Dr. D. S. Bayard at the Jet Propulsion Laboratory, Pasadena, California who provided the experimental data from the ARC testbed.

References

[1] M. Moonen, B. De Moor, L. Vandenberghe, and J. Vandewalle, "On- and off-line identification of linear state-space models," *Int. J. Control*, vol. 49, no. 1, pp. 219–232, 1989.

[2] P. Van Overschee and B. De Moor, "N4SID: Subspace algorithms for the identification of combined deterministic-stochastic systems," *Automatica*, vol. 30, no. 1, pp. 75–93, 1994.

[3] M. Verhaegen, "Subspace model identification, Part III: Analysis of the ordinary output-error state space model identification algorithm," *Int. J. Control*, vol. 58, pp. 555–586, 1993.

[4] ——, "Identification of the deterministic part of MIMO state space models given in innovations form from input-output data," *Automatica*, vol. 30, no. 1, pp. 61–74, 1994.

[5] M. Viberg, "Subspace-based methods for the identification of linear time-invariant systems," *Automatica*, vol. 31, no. 12, pp. 1835–1851, 1995.

[6] L. Ljung, *System Identification: Theory for the User*, 2nd ed. Englewood Cliffs, New Jersey: Prentice-Hall, 1999.

[7] R. Pintelon and J. Schoukens, *System Identification - A frequency domain approach*. IEEE Press, 2001.

[8] K. Liu, R. N. Jacques, and D. W. Miller, "Frequency domain structural system identification by observability range space extraction," in *Proc. American Control Conference, Baltimore, Maryland*, vol. 1, June 1994, pp. 107–111.

[9] T. McKelvey, H. Akçay, and L. Ljung, "Subspace-based multivariable system identification from frequency response data," *IEEE Trans. on Automatic Control*, vol. 41, no. 7, pp. 960–979, July 1996.

[10] T. McKelvey, A. Fleming, and R. S. O. Moheimani, "Subspace-based system identification of an acoustic enclosure," *ASME Transactions of Vibration and Acoustics*, vol. 124, no. 3, July 2002.

[11] P. Van Overschee and B. De Moor, "Continuous-time frequency domain subspace system identification," *Signal Processing, EURASIP*, vol. 52, no. 2, pp. 179–194, July 1996.

[12] T. Kailath, *Linear Systems*. Englewood Cliffs, New Jersey: Prentice-Hall, 1980.

[13] T. McKelvey, "On the finite length DFT of input-output signals of multivariable linear systems," in *Proc.of 39th Conference on Decision and Control*, vol. 5, Sydney, Australia, Dec 2000, pp. 5190–5191.

[14] G. H. Golub and C. F. Van Loan, *Matrix Computations*, 2nd ed. Baltimore, Maryland: The Johns Hopkins University Press, 1989.

[15] A. Graham, *Kronecker Products and Matrix Calculus With Applications*. Chichester, England: Ellis Horwood Limited, 1981.

[16] R. Pintelon, "Frequency-domain subspace system identification using non-parametric noise models," *Automatica*, vol. 38, pp. 1295–1311, 2002.

[17] U. M. Al-Saggaf and G. F. Franklin, "Model reduction via balanced realizations: An extension and frequency weighting techniques," *IEEE Trans. on Automatic Control*, vol. 33, no. 7, pp. 687–692, July 1988.

[18] T. McKelvey, "Frequency domain identification," in *Preprints of the 12th IFAC Symposium on System Identification*, R. Smith and D. Seborg, Eds., Santa Barbara, CA, USA, June 2000, plenary paper.